CEMENT and CONCRETE RESEARCH. Vol. 12, pp. 209-226, 1982. Printed in the USA.
0008-8846/82/020209-18$03.00/0 Pergamon Press, Ltd.

EFFECT OF CRACKING IN DRYING AND SHRINKAGE SPECIMENS

Zdeněk P. Bažant* and Warren J. Raftshol**
Center for Concrete and Geomaterials
The Technological Institute, Northwestern University
Evanston, Illinois 60201, U.S.A.

(Communicated by F.H. Wittmann)
(Received Oct. 26, 1981)

ABSTRACT

The significance of cracking and microcracking caused by nonuniform drying shrinkage of test specimens is analyzed. To assure that no cracks are produced by drying in load-free specimens, one must lower the environmental humidity gradually and sufficiently slowly, and use very thin specimens (about 1 mm thick). Graphs for the maximum admissible rate of change of environmental humidity, calculated from both linear and nonlinear diffusion theories, are provided. The spacing and width of parallel cracks due to drying are estimated from fracture mechanics considerations. In normal size specimens the drying cracks are usually too narrow to be visible. Drying leads to discontinuous microcracking rather than continuous macrocracks and is represented better as strain softening than as an abrupt stress drop. Shrinkage cracking can increase drying diffusivity by several orders of magnitude.

RESUME

On étudie l'importance de la fissuration et de la microfissuration d'éprouvettes soumises au retrait de séchage non-uniforme. Pour éviter les fissures dues au séchage dans les éprouvettes non-chargées, il faut reduire l'humidité environnante graduellement et suffisamment lentement, et il faut ululiser des éprouvettes très minces (environ 1 mm d'épaisseur). On donne des graphiques pour le taux maximum de réduction de l'humidité environnante, calculé d'aprés les théories linéaire ainsi que non-linéaire, de diffusion. A l'aide de la mécanique de rupture, on estime l'espacement et la largeur des fissures parallèles dues au séchage. Dans les éprouvettes de dimensions normales, les fissures de séchage sont généralement trop minces pour être visibles. Le séchage provoque une microfissuration discontinue, plutôt que des macrofissures continues, et on le décrit mieux par une relation contrainte-déformation à pente négative (radoucissement) que par une perte soudaine de la contrainte. Les fissures de retrait peuvent augmenter la diffusivité de séchage de plusieurs ordres de grandeur.

---

*Professor of Civil Engineering and Director.
**Graduate Research Assistant.

Introduction

Shrinkage caused by drying is known to be capable of producing cracks in concrete specimens as well as structures. The cracks alleviate the stresses due to differential strains and thus they alter the observed deformations. Furthermore, the presence of cracks may increase the rate of drying. Although the existence of these effects is well known, their significance for the conduct of drying and shrinkage tests is not fully appreciated. Interpretation of many of the experimental results in the literature is dubious due to lack of separation of the effects of cracking and microcracking.

The formation of tensile microcracks in shrinkage and creep specimens was taken into account by means of tensile nonlinearity in the finite element model in Ref. [1] which was used to analyze numerous creep and shrinkage test data. Becker and Bresler [2] included tensile cracking in their finite element analysis of creep, shrinkage and thermal stresses in concrete columns subjected to fire. A profound investigation of the effect of tensile cracking in separating measured deformations into creep and shrinkage was presented by Wittmann and Roelfstra [3]. Their investigation showed that much of the drying creep effect, i.e., the increase of creep of test specimens caused by simultaneous drying, may be attributable to the effect of cracking rather than some mechanism on the molecular level.

For direct determination of the properties of the drying material as such, tests must be arranged so as to avoid cracking. The conditions under which this is achieved will be analyzed in this study.

Estimate of Maximum Pore Humidity Difference

The free (i.e. unrestrained) shrinkage ε_S of a small element of concrete, caused by a decrease of pore humidity from 1 to h is a function of h. Approximately we may write [4]

$$\varepsilon_S = \varepsilon_S^0 f_S(h) \cong \varepsilon_S^0(1 - h^3) \tag{1}$$

where ε_S^0 = shrinkage upon complete drying (at no cracking!). The slope of the curve $1 - h^3$ is the greatest in the vicinity of saturation (h = 1), for which maximum effect of differential shrinkage is to be expected. For the vicinity of h = 1 Eq. (1) may be replaced by a tangent at h = 1, for which

$$\varepsilon_S \cong 3\varepsilon_S^0(1 - h). \tag{2}$$

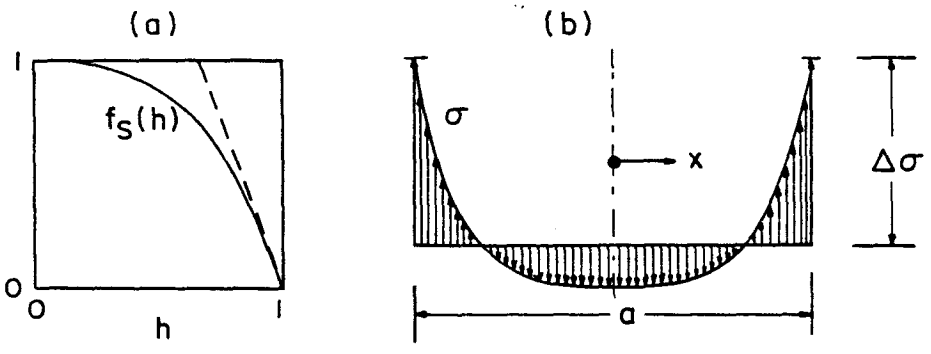

FIG. 1

Variation of Free Shrinkage with Relative Humidity h in Pores (a), and Typical Distribution of Shrinkage Stresses throughout a Wall (b).

In an infinitely long wall or cylinder, the actual longitudinal strain must be constant across the thickness (due to translation symmetry) and, approximately, this condition may be assumed even for a wall or cylinder of a finite length. The longitudinal normal stresses σ, which are produced by shrinkage (shrinkage stresses), may be determined from the conditions that the strain must be uniform and the axial resultant of the stresses over the cross section must be zero. The typical distributions of shrinkage stress obtained by such a calculation [4,2,3] are shown in Fig. 1(b). As long as the humidity within the cross section is close to 1.0, the difference between the maximum stress and minimum stress is approximately (in absence of cracking)

$$\Delta\sigma = 3\varepsilon_s^0(1 - h)E_{eff} \tag{3}$$

where E_{eff} = effective modulus = Young's modulus E reduced to take into account the creep. For sudden exposure to the environment, the largest shrinkage stresses are produced near the surface right at the beginning, in which case the drying period is so short that the reduction of E due to drying is negligible (compared to the conventional value of E) and we may use $E_{eff} = E$.

The maximum tensile stress σ_{max} is always less than $\Delta\sigma$ but often is rather close to σ_{max} (see Fig. 1b); we therefore assume that $\sigma_{max} \approx 0.9\ \Delta\sigma$. To avoid cracking, σ_{max} must not exceed the uniaxial tensile strength f_t'. The strength depends on the stress duration $t - t_0$, but again, for very thin specimens the use of the short-time strength is appropriate. To avoid tensile nonlinear behavior (microcracking), σ_{max} should be less than about $0.7\ f_t'$ for concrete and $0.9\ f_t'$ for cement paste.

The maximum admissible pore humidity difference between the center and the surface of the specimen may now be estimated as $\Delta h_{max} = \text{Max}(h_c - h_s) = \Delta\sigma/(3\varepsilon_s^0 E_{eff})$, where $\Delta\sigma = \sigma_{max}/0.9$, $\sigma_{max} = 0.7\ f_t'$, i.e.,

$$\Delta h_{max} \approx \frac{0.26\ f_t'}{\varepsilon_s^0 E_{eff}} \tag{4}$$

for the most unfavorable situation at the start of drying, and the surface layer of concrete. For hardened cement paste specimens we may use $\Delta\sigma \approx 0.9\ f_t'$ which yields coefficient 0.33 instead of 0.26.

To make a numerical estimate, we should note that the final free shrinkage (in absence of cracking) might be at most about 33% larger than the shrinkage measured by conventional tests, in which the specimen shrinkage is reduced by microcracking. For most structural concretes, the final shrinkage ranges from 0.0004 to 0.0011, and so a safe limit for all cases is $\varepsilon_s^0 = 1.33 \times 0.0011 \approx 0.0015$. Taking further $E = 4 \times 10^6$ psi (27,600 N/mm^2) and $f_t' = 425$ psi (2.93 N/mm^2), we get

$$\Delta h_{max} = 0.018 \tag{5}$$

as the maximum pore humidity difference within the cross section which we may consider safe (although often, perhaps, not necessary) to avoid cracking and microcracking in the surface layer of concrete.

This estimate is surprisingly restrictive. It was certainly based on extreme properties. E.g., if $\varepsilon_s^0 = 0.0004$, we have $\Delta h_{max} = 0.066$ for the surface layer of concrete; and for concrete several inches below the surface this limit may be about doubled, $\Delta h_{max} = 0.11$, due to a longer drying period (creep) and the fact that the critical humidity range is not close to 1.0.

For pure hardened cement paste the limit on Δh is even stricter. The shrinkage is about 5 times larger than for concrete, E is about 33% less, and

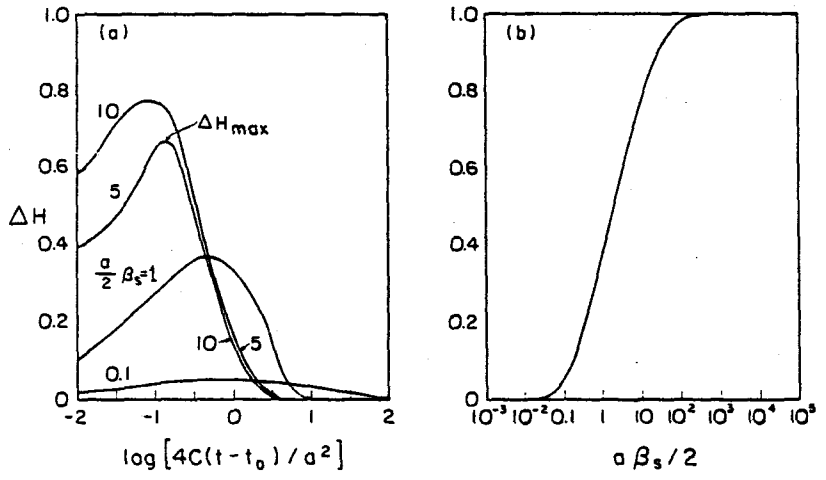

FIG. 2

Difference in Humidity Parameters H between Center and Surface of Wall of Thickness a after Sudden Exposure to Constant Humidity Environment (β_S = surface emissivity of moisture; ΔH_{max} = maximum of ΔH in time).

$\sigma_{max} = 0.9\, f_t'$. This yields $\Delta h_{max} = 0.006$ as the overall sufficient limit for the pore humidity differences to avoid cracking.

Sudden Exposure to Environmental Humidity at Finite Surface Emissivity

The one-dimensional diffusion equation which governs drying of a concrete wall or cylinder at constant temperature may be written as follows:

$$\frac{\partial h}{\partial t} = \frac{\partial}{\partial x}\left(C\,\frac{\partial h}{\partial x}\right) \quad \text{or} \quad \frac{\partial h}{\partial t} = \frac{1}{r}\,\frac{\partial}{\partial r}\left(Cr\,\frac{\partial h}{\partial r}\right). \tag{6}$$

Here x is the coordinate across the thickness of the wall, r is the radial coordinate (see Fig. 3), t = time, h = relative pressure of water vapor in the capillary pores, and C = diffusivity of concrete, which is known to be strongly dependent on h and to approximately follow the relation [5]

$$C = C_1 f(h') = C_1\left(\alpha_0 + \frac{1-\alpha_0}{1-h'^{n}}\right), \quad h' = \frac{1-h}{1-h_c} \tag{7}$$

in which C_1 = constant = diffusivity at saturation (h = 1), and n, α_0, h_c = material constants, $n \simeq 4$, $\alpha_0 \simeq 0.05$, $h_c \simeq 0.75$ [5]. For crude approximate calculations it is possible to replace variable C with a constant value C equal to about 1/4 of C_1. This makes the diffusion problem linear.

As the initial conditions we consider:

$$\text{for } t = t_0 \text{ and } -\frac{a}{2} \le x \le \frac{a}{2} \quad \text{or} \quad 0 \le r \le a: \quad h = 1 \tag{8}$$

where a = thickness of wall or radius of cylinder. The boundary condition on a free surface in contact with an environment of relative vapor pressure $h = h_e$ may be written as

$$\text{for } x = \pm\frac{a}{2} \text{ or } r = a \text{ and } t > t_0: \quad \frac{\partial h}{\partial x} = \beta_S(h_e - h) \quad \text{or} \quad \frac{\partial h}{\partial r} = \beta_S(h_e - h) \tag{9}$$

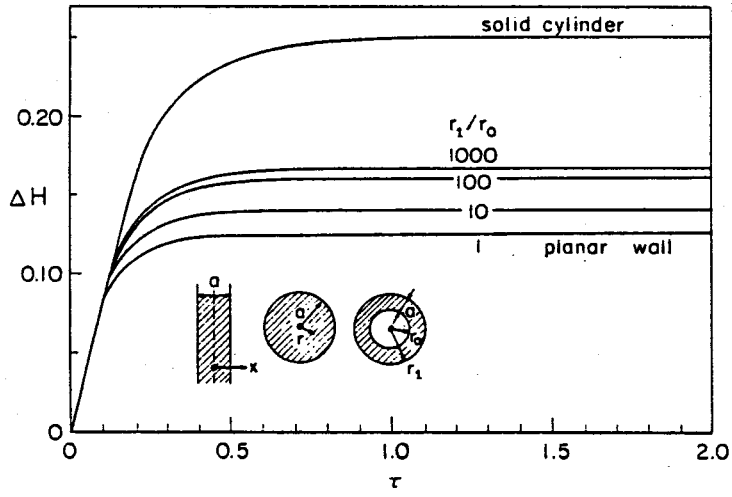

FIG. 3

Maximum Lag of Humidity Parameter ΔH within the Specimen Behind Its Surface Value H_c for Linear Variation of H_e and Constant Diffusivity C.

where β_S = given surface emissivity of moisture.

Certain properties of the solution can be made obvious by introducing new variables as follows:

$$\xi = \frac{x}{a} \text{ or } \frac{r}{a}, \quad \tau = \frac{C_1}{a^2}(t - t_0), \quad H = \frac{1 - h}{1 - h_e}. \tag{10}$$

Eq. (6) then yields the differential equation:

$$\frac{\partial H}{\partial \tau} = \frac{\partial}{\partial \xi}\left(f(h')\frac{\partial H}{\partial \xi}\right) \quad \text{or} \quad \frac{\partial H}{\partial \tau} = \frac{1}{\xi}\frac{\partial}{\partial \xi}\left(f(h')\,\xi\,\frac{\partial H}{\partial \xi}\right), \tag{11}$$

with
$$h' = \frac{1 - h_e}{1 - h_c} H. \tag{12}$$

The initial condition (Eq. 8) becomes

$$\text{for } \tau = 0 \text{ and } -\tfrac{1}{2} \le \xi \le \tfrac{1}{2} \text{ or } 0 \le \xi \le 1: \quad H = 0 \tag{13}$$

and the boundary conditions (Eqs. 9) become:

$$\text{for } \xi = \pm\tfrac{1}{2} \text{ or } \xi = 1 \text{ and } \tau > 0: \quad \frac{\partial H}{\partial \xi} = a\beta_S(1 - H). \tag{14}$$

We see that the boundary conditions for the function $H(\xi,\tau)$ involve only one parameter, $a\beta_S$. The solution $H(\xi,\tau)$ depends only on the following variables:

$$\xi,\ \tau,\ a\beta_S; \text{ and } \frac{1 - h_e}{1 - h_c},\ \alpha_0\ . \tag{15}$$

The last two parameters, which are needed only for calculation of f(h') in Eqs. (11) and (7), disappear when the diffusivity is considered to be constant. According to Eq. (7), the solution depends also on the parameter $(1-h_e)/(1-h_c)$, since this parameter is needed to determine function f(h') in Eq. (11).

For the case f(h') = const. = 1, for which the diffusion problem is

linear, the solution of the foregoing problem is available in the form of a series [6]. For our purpose, it is of interest to determine the difference ΔH between the maximum and the minimum value of H throughout the thickness. Here we have $\Delta H = H_s - H_c$, where H_c and H_s = values of H at the center ($\xi = 0$) and at the surface ($\xi = 1$ or $\xi = \pm \frac{1}{2}$). From Figs. 17 and 18 of Ref. [6] one can construct for the case of constant diffusivity the diagram of $\Delta H = H_s - H_c$ versus τ at various values of $a\beta_S$. This diagram is shown in Fig. 2(a). We see that the maximum of ΔH, represented by the peaks of the curves in Fig. 1(a), is independent of diffusivity C and depends strongly on the parameter $a\beta_S$; we plot this dependence in Fig. 2(b).

Consider now drying at environmental humidity $h_e = 50\%$. Then $H = 2(1-h)$ and since the maximum difference in h throughout the cross section is 0.018 (Eq. 5) if cracking should be avoided, the maximum difference in H is 0.036. From Fig. 2(b) we see that to assure $\Delta H \leq 0.036$ we need that

$$a \leq 0.1/\beta_S. \tag{16}$$

Now we have to choose a realistic value for the surface emissivity of moisture, β_S. Its value is known to vary by an order of magnitude depending on air circulation, particularly the velocity of air flow past the surface. The value $1/\beta_S$ is called the equivalent surface thickness [5] since it represents the thickness of a layer of material on which the humidity drop in a steady state permeation is equal to the surface drop. Aleksandrovskii [7] indicates $1/\beta_S \approx 20$ to 100 mm, but this value has apparently been inferred from tests on thick specimens which can easily lead to considerable error. Indirect evidence in Ref. [5] suggests a much smaller value of $1/\beta_S$ for typical laboratory specimens, $1/\beta_S \approx 1$ mm, and maybe even less. If the latter value is correct, then the maximum half-thickness of wall for which a sudden response to the environment of $h_e = 50\%$ would not produce cracking or microcracking is

$$a_{max} \approx 0.1 \text{ mm}. \tag{17}$$

This is a practically unsatisfiable limitation.

It has been sometimes assumed that the free shrinkage may be determined by testing specimens of different wall thickness and extrapolating the results to zero thickness. There are, however, limitations on the wall thicknesses that can be used for this purpose. To admit extrapolation, all data points must correspond to the steadily rising part of the curve in Fig. 2(b), which corresponds to $0.2 \leq a\beta_S \leq 50$. Taking $1/\beta_S = 1$ mm, we thus have the limitation

$$0.2 \text{ mm} \leq a \leq 50 \text{ mm}. \tag{18}$$

These sizes are too small for concrete compared to the size of aggregate, and so its free shrinkage cannot be determined in this manner.

For hardened cement paste, the range indicated by Eq. (18) is acceptable. This lends support to extrapolations to zero thickness carried out by Klug [8]. However, one must be cautious with regard to the value of β_S. It may be as small as 0.1 mm and then the range would be $0.02 \text{ mm} \leq a \leq 5$ mm, which would be unacceptably small even for cement paste.

The foregoing crude analysis was based on linear diffusion theory (constant C). The nonlinear diffusion theory, for which the solution would have to be obtained numerically, would no doubt yield results that do not differ in their order of magnitude, which is all that we aim for here.

For specimen sizes above the transition zone in Fig. 2(b) (Eq. 18), i.e., for values of a in excess of 20 mm and perhaps even 2 mm, Δh_{max} is almost

equal to $1-h_e$. We may then assume perfect moisture transmission at the surface, i.e., $1/\beta_S = 0$, in which case the boundary condition is that of prescribed humidity:

$$\text{for } x = \pm\frac{a}{2} \text{ or } r = a \text{ and } t > t_0: \quad h = h_e. \tag{19}$$

In our further analysis we will assume this boundary condition.

Gradual Decrease of Environmental Humidity

Pore humidity differences which avoid cracking can be obtained for concrete if the environmental humidity is decreased gradually. We consider a ramp history in which h is decreased from h = 1 linearly until a constant value h_1 is reached, and we consider a planar wall of thickness 2a, or solid cylinder of radius r_1, or hollow cylinder of external radius r_1 and internal radius r_0. Then, assuming a perfect moisture transfer at the surface, we have

$$\left.\begin{aligned} &x = \pm a/2 \\ \text{or } &r = r_1 \\ \text{or } &r = r_0 \text{ and } r = r_1 \end{aligned}\right\} \quad \begin{aligned} t_0 \le t \le t_1: &\quad h = 1 - k(t - t_0) \\ t \ge t_1: &\quad h = h_1 - \text{const.} \end{aligned} \tag{20}$$

The initial condition and the governing differential equation are again given by Eqs. (8) and (6). Introducing new nondimensional variables as in Eq. (10),

$$\xi = \frac{x}{a} \text{ or } \frac{r}{r_1}, \quad \tau = \frac{C_1}{a^2}(t - t_0), \quad H = \frac{C_1}{a^2 k}(1 - h) \tag{21}$$

the differential equation for $H(\xi,\tau)$ is given by Eq. (11) with

$$h' = \frac{a^2 k}{C_1(1 - h_c)} H. \tag{22}$$

The initial condition is given by Eq. (13), and the boundary conditions are:

$$\left.\begin{aligned} &\text{for } \xi = \pm\tfrac{1}{2} \\ &\text{or } \xi = 1 \\ &\text{or } \xi = 1 \text{ and } \xi = r_0/r_1 \end{aligned}\right\} \quad \begin{aligned} 0 < \tau \le \tau_1: &\quad H = \tau \\ \tau \ge \tau_1: &\quad H = \frac{C_1}{a^2 k}(1 - h_1) \end{aligned} \tag{23}$$

where $\tau_1 = C_1(t_1 - t_0)/a^2$. We see that the solution $H(\xi,\tau)$ depends only on the variables:

$$\xi, \ \tau, \ \frac{C_1(1 - h_1)}{a^2 k}; \quad \text{and} \quad \frac{C_1(1 - h_c)}{a^2 k}, \ \alpha_0. \tag{24}$$

The last two parameters disappear when the diffusivity is considered to be constant. This is the case of linear diffusion theory (which is equivalent to $\alpha_0 \to 1$).

For the linear diffusion theory, the solution may be obtained by superposition, integrating the series solution for a step change of surface humidity [6]. This yields the series solution given in the Appendix (Eq. 46). For hollow cylinders the series is involved, and it was more convenient to use the finite difference Crank-Nicholson algorithm. From these solutions, we can calculate the maximum humidity difference Δh in the cross section at any given time; $\Delta h = h_m - h_s$, where h_m = humidity at the center and h_s = humidity at the surface. The plot of parameter $\Delta H = (C_1/a^2 k)\Delta h$ versus nondimensional time τ is given in Fig. 3, in which a represents the effective thickness, defined as the cross sectional area divided by the exposed perimeter (or volume-to-surface

ratio); for a slab, a = thickness; for a solid cylinder, a = r_1 = radius; and for a hollow cylinder, a = $r_1 - r_0$ = wall thickness.

For the nonlinear diffusion theory (variable C), the solutions have been obtained numerically, using finite differences (Lees' method). The numerical results are plotted in Fig. 4(a-d) for various values of parameter $\kappa = (a^2k)/C_1(1-h_c)$. (The case $h_c \to -\infty$ or $\kappa \to 0$ represents the linear diffusion theory, Fig. 3.)

Subsequent to the end of the ramp, t_1, i.e., after h reaches h_1, the humidity difference Δh always decreases. From $t = t_0$ to $t = t_1$, Δh monotonically increases. These facts can be easily verified from the series expression given in the Appendix for the case C = const. So, the maximum Δh occurs at the end of the ramp, $t = t_1$. If time t_1 is increased, Δh tends asymptotically to a constant. From Figs. 3 and 4 we find that the asymptotic value is closely approached if

$$\frac{C}{a^2}(t - t_0) \geq 0.7 \quad \text{(constant C)} \tag{25a}$$

$$\frac{C_1\alpha_0}{a^2}(t - t_0) \geq 2 \quad \text{(all cases of variable C).} \tag{25b}$$

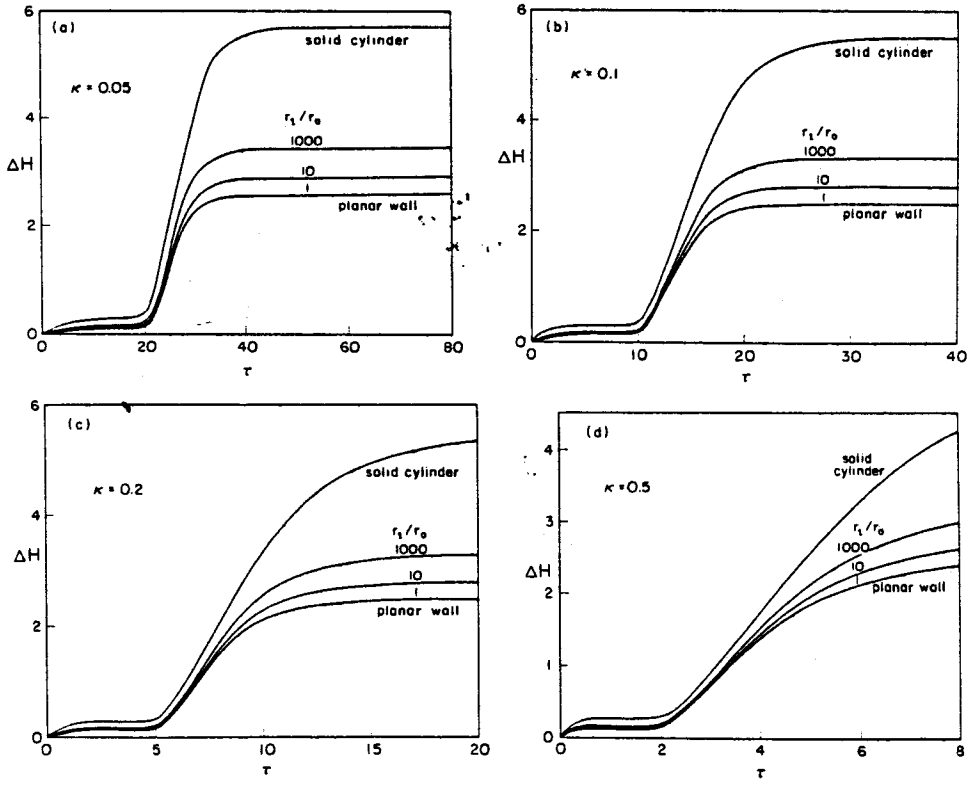

FIG. 4

Lag of Humidity Parameter H within the Specimen behind Its Surface Value H_e for Linear Variation of H_e and Variable Diffusivity C (Eq. 7)

What is the maximum rate of humidity change for which cracking and microcracking are avoided? We can now answer this question with the help of the graphs in Figs. 3 and 4. Consider a planar wall and linear diffusion theory (constant C) and assume that the humidity change is sufficiently slow so that the end of the ramp (time t_1) satisfies Eq. (25a,b). Then, from Fig. 3 $\Delta hC/ka^2 = 0.125$. Substituting $\Delta h = \Delta h_{max} = 0.018$ (Eq. 5), we have

$$\text{Max } k = 0.14\ C/a^2. \tag{26}$$

We may now check whether this humidity rate is sufficient to reach the end of the ramp, $t = t_1$. We consider drying from 100% to 50% humidity, for which $k = 0.5/(t - t_0)$. Eq. (26) then yields $(C/a^2)(t-t_0) = 0.5/0.14 > 0.7$. So, this humidity rate is sufficient to reach the asymptotic Δh before constant h is reached.

For a typical structural concrete we may now consider $C = 10$ mm^2/day. For a 6 inch (15 cm) wall we get the maximum as $k \approx 6\times10^{-5}$/day, which means that the humidity decrease from 100% to 50% would have to be made gradually over the period of 23 years in order to be sure of avoiding cracking and microcracking. For a 0.75 mm wall thickness and same C [9], Eq. (26) indicates that the decrease from 100% to 50% would have to be made over the period of 5 hours, which is roughly what was used in the tests reported in Ref. [9]. For the nonlinear diffusion theory, the results are of the same order of magnitude.

From the foregoing analysis it is clear that in conventional tests the cracking and microcracking can be avoided only for ultra-thin cement paste specimens (about 1 mm). It was for this reason that these ultra-thin specimens were developed for the study in Ref. [9]. For concrete and mortar, drying tests cannot be carried out without causing the specimen to crack or microcrack.

The foregoing conclusion puts in question the interpretation of many drying and shrinkage tests carried out in the past. There has been a tendency to jump from observations of moisture losses and dimensional changes to explanations in terms of molecular mechanisms, while microcracking and possibly even continuous cracking must have often significantly affected the results. If a sufficiently slow variation of environmental humidity is unacceptable, the cracking can be avoided only by applying loads which produce sufficient compressive stresses. A large enough axial compression on a cylinder prevents cracking in the planes normal to the axis, but does not prevent cracking in the radial or tangential planes. The normal stresses caused by drying in the radial planes are about the same as those in the axial planes [1]. Furthermore, the measurements on a companion load-free specimen are normally used to determine the magnitude of load-produced creep, and these measurements are affected by cracking.

Spacing and Width of Macroscopic Cracks

Drying typically produces systems of parallel cracks (Fig. 5). For estimating various consequences of cracking, the crack spacing and the crack width need to be known. Both problems are related; if the crack spacing s is known, then the crack width w can be easily estimated.

The first problem of crack spacing is that of initial spacing when the first parallel cracks are formed. A second problem is then the formation of secondary cracks or the closing of the previously formed cracks. The problem of crack spacing has been solved [11,12] for a homogeneous elastic halfspace cooled from its surface, the boundary condition consisting of given constant surface temperature. This problem is equivalent to that of shrinkage of the

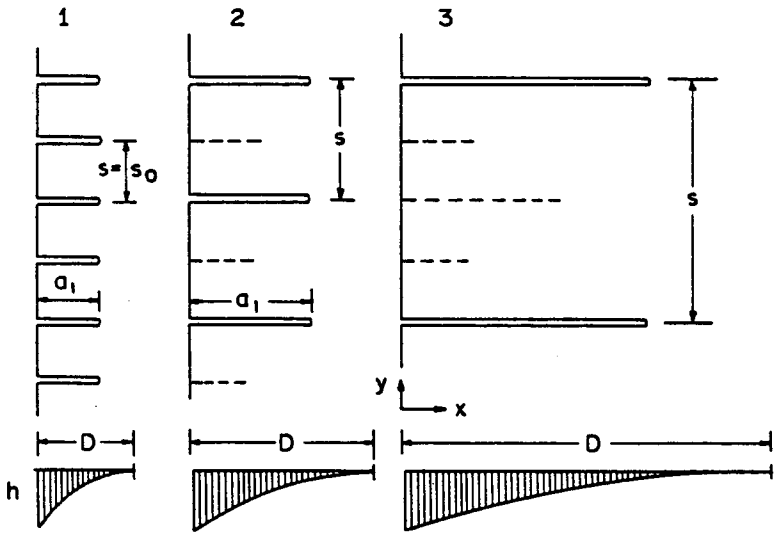

FIG. 5

Crack Closing and Doubling of Spacing in a System of Parallel Drying Cracks in a Halfspace.

halfspace due to drying from the surface (provided that linear elasticity and linear diffusion theory are assumed). A lower bound on the initial spacing of normal cracks in an elastic halfspace may be obtained by the use of fracture mechanics, expressing the fact that the fracture energy needed to produce the cracks cannot exceed the strain energy in the halfspace before cracking. This condition yields the formula [11,12]

$$s \geq \frac{10(1-\nu)a_1 G_{fr}}{(1+\nu)\Delta\varepsilon_{sh}^2 D E} \tag{27}$$

in which $\Delta\varepsilon_{sh}$ = free shrinkage strain in the halfspace, G_{fr} = specific fracture energy = energy needed to produce a crack of unit length (or unit area), E = Young's elastic modulus, ν = Poisson's ratio, a_1 = length of the cracks, D = penetration depth of the drying front. According to the solution in Refs. [11-13], we may substitute $a_1/D \approx 1.5$. Then, using for concrete typical values $G_{fr} \approx 50$ N/m [15-18], $E = 3\times10^4$ MN/m^2, $\Delta\varepsilon_{sh} = 6\times10^{-4}$ and $\nu = 0.18$, we get

$$s \geq 48 \text{ mm} \quad (\text{for } a_1 \geq 100 \text{ mm}). \tag{28}$$

This calculation makes sense only if the cracks are several times longer than the aggregate size, and for this reason we impose the limit $a_1 \geq 100$ mm. For cement paste we may use $G_{fr} \approx 15$ N/m, $\Delta\varepsilon_{sh} \approx 12\times10^{-4}$, and thus we get

$$s \geq 3 \text{ mm} \quad (\text{for } a_1 \geq 10 \text{ mm})$$

where we indicate a lower limit on crack length a_1 (10 mm) because the inhomogeneities in cement paste are of much smaller size than in concrete.

Since the first cracking relieves most of the strain energy initially contained in the halfspace, these formulas may be regarded not only as lower bounds but also as approximate estimates. For walls of finite thickness, the solution has not yet been carried out but the foregoing formulas probably als

give reasonable estimates for cracks through part of the wall thickness. The foregoing values apply only to unreinforced specimens. Some solutions for reinforced concrete were given in Ref. [13].

Since the normal stress parallel to the halfspace surface is almost completely relaxed by cracking, the width of the cracks at their mouth is

$$w = s\Delta\varepsilon_{sh}. \tag{29}$$

For the previously used material characteristics, we then get

$$\begin{aligned} &\text{for concrete:} \quad w \approx 6\times10^{-4}\times 48 \text{ mm} = 0.03 \text{ mm} \\ &\text{for cement paste:} \quad w \approx 12\times10^{-4}\times 3 \text{ mm} = 0.004 \text{ mm} \end{aligned} \tag{30}$$

Cracks as fine as this are obviously not visually detectable by the unaided eye.

The evolution of the crack system subsequent to the first cracking has also been solved on the basis of fracture mechanics and stability analysis [11-13]. Surprisingly, further penetration of the drying front into the halfspace does not increase the number of cracks. Rather, every other crack closes, with the effect that the spacing and the width of the open cracks doubles. More precisely, at a certain critical length a_1^{cr}, the parallel cracks reach a state of instability in which every other crack suddenly jumps ahead at constant loading (constant D), and the intermediate cracks begin to close (i.e., their stress intensity factor drops below its critical value). Later, as the drying penetrates deeper and the open cracks advance farther, the intermediate cracks close completely, the spacing of the open cracks thus being doubled. As these open cracks extend further, a similar instability occurs again, the spacing of open cracks being doubled the second time, etc. The length of the open cracks is found [11-12] to fluctuate between

$$0.67D \leq a \leq 0.77D \tag{31}$$

where the first limit corresponds to the start of closing of every other crack, and the second limit to the completion of their closing. The corresponding fluctuation of the spacing of open cracks is within the limits

$$0.39D \leq s \leq 0.61D. \tag{32}$$

According to inequalities (31) and (32), the average crack length and crack spacing may be expressed as

$$a \approx 0.72D, \quad s \approx 0.69a = 0.5D. \tag{33}$$

From these relations we see that the open shrinkage cracks get more widely spaced and more widely opened as the drying front penetrates into a wall. For the cracks to become visible to an unaided eye, their width must be at least 0.2 mm, which occurs for

$$s \geq 30 \text{ cm}, \quad D \geq 60 \text{ cm}, \quad a \geq 43 \text{ cm} \tag{34}$$

if $\Delta\varepsilon_{sh} = 6\times10^{-4}$. The required value D = 60 cm is so large that a system of parallel drying cracks cannot normally be visible in normal size concrete (as well as cement paste) specimens.

Cracks of other types may, however, occur and be easily visible in rather small specimens. For example, an ultra-thin tubular cement paste specimen [9], if suddenly exposed to a room environment of relative humidity around 60%, fails suddenly by a single crack through the entire thickness of the wall, parallel to the axis. The energy to produce this crack must come from the bending energy of the thin-wall tube due to warping from nonuniform shrinkage. We assume the more critical case when a tube dries only from the outside (at constant h_e) rather than from both surfaces, and consider the distribution of

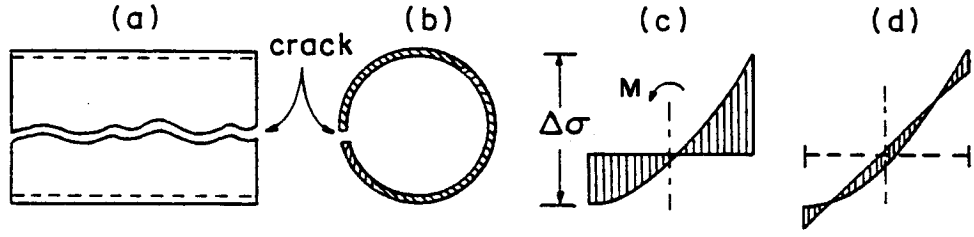

FIG. 6

Longitudinal Cracking of Thin-Walled Tubular Drying Specimen

normal stress due to shrinkage to be parabolic (Fig. 6c), with the drying front just reaching the inside face. The bending moment of this stress distribution about the midthickness of wall is $M = \Delta\sigma\, a^2/12$ where $\Delta\sigma = E'(1+\nu)\Delta\varepsilon_{sh}$, $E' = E/(1-\nu^2)$. The formation of the longitudinal crack relieves the entire energy of circumferential bending of the tube, and so $U = 2\pi r M^2/(2E'I)$, $I = a^3/12$ (per unit length of the tube) where r = radius of the mid-surface of the wall. This must equal the fracture energy, i.e. $U = G_{fr}a$, which yields

$$\Delta\varepsilon_{sh} = \left(\frac{1-\nu}{1+\nu}\,\frac{12G_{fr}}{\pi rE}\right)^{\frac{1}{2}} \tag{35}$$

as the critical shrinkage strain which is capable of causing the crack. Considering $G_{fr} \approx 10$ N/m (cement paste), $E = 2\times10^4$ MN/m^2, $r = 7.5$ mm, and $a = 0.75$ mm, we then get $\Delta\varepsilon_{sh} = 0.00042$. Assuming $\varepsilon_s^0 = 0.0015$, this critical value would be attained by an abrupt exposure to environmental humidity $h_e = 0.90$. Indeed, a sudden exposure of thin-wall tubes to this humidity has been observed to cause a crack [9,19].

Cracks of this type do not, however, endanger the correctness of interpretation of tests since the experimentalist is aware of them.

Discontinuous Microcracks

The previous analysis of crack spacing is contingent upon the applicability of fracture energy values G_{fr} known from fracture testing. Physically, G_{fr} represents the surface energy of a wide band of microcracks that must form ahead of the crack front if the fracture should advance. The energy of formation of individual microcracks, to which we now turn our attention, is obviously much smaller. No direct experimental evidence exists for the value of this energy, and so we will approach the microcrack formation in a different manner.

Under tensile stresses, all of the inelastic strain is due to the formation of microcracks. Assuming that there is complete biaxial restraint, and that the biaxial tensile strength equals the uniaxial tensile strength f_t', the elastic strain parallel to the surface of concrete is at most $f_t'(1-\nu)/E_c$.

The total strain caused by the stress is at most (for total restraint) $\Delta\varepsilon_{sh}$, and so the total strain due to microcracking is $\Delta\varepsilon_{cr} = \Delta\varepsilon_{sh} - f_t'(1-\nu)/E_c$. Hence the volume of microcracks per unit volume of the material may be approximated as

$$\Delta v_{cr} = 2\left(\Delta\varepsilon_{sh} - \frac{f_t'(1-\nu)}{E_c}\right). \tag{36}$$

Then, if we would know the mean spacing of microcracks, s, and if the microcracks were of two directions, the crack width would be

$$w = \tfrac{1}{2} v_{cr} s. \tag{37}$$

As typical values we may consider $\Delta\varepsilon_{sh} = 6\times10^{-4}$, $f_t' = 3.45$ N/mm^2 (500 psi), $E_c = 27800$ N/mm^2 (4×10^6 psi), $\nu = 0.18$, and assume that $s \leq 1$ cm. This then yields $\Delta v_{cr} = 0.001$ and

$$w \leq 0.005 \text{ mm} \tag{38}$$

as the maximum width of the microcracks. Such microcracks are obviously not visible to the naked eye. However, such microcracks were observed by scanning electronic microscopy by Mindess and Diamond [20]; their width was indeed of the order of a few microns.

Based on the preceding analysis, microcracks (rather than macrocracks) must be expected to form when the penetration of the drying front is less than about 60 cm from the surface, which is typically the case in all test specimens. Microcracking is not very well modeled by assuming a sudden drop of the stress to zero. Rather, microcracks develop gradually and cause gradual strain softening (negative slope) in the stress-strain relation (Fig. 7). For the analysis of measurements on standard test specimens it is therefore more realistic to assume tensile strain softening rather than a sudden complete cracking. It was for this reason that a tensile nonlinearity rather than cracking was assumed in analyzing the shrinkage and creep test data in Ref. [1]. From the viewpoint of convenience, however, it may be simpler to consider cracking because the three-dimensional tensorial properties of the strain-softening tensile stress-strain relations are not too well understood at present. Perhaps the error caused by the consideration of sudden cracking instead of gradual strain softening is not too large.

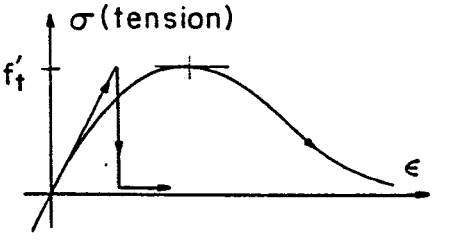

FIG. 7

Models of Tensile Stress-Strain Diagram — Cracking and Gradual Strain Softening

Another question of interest is whether the microcracking produced by drying can significantly affect the measured internal surface area. Its magnitude for hardened cement paste is of the order of 500 m^2 per cm^3 of material. For the microcracking to have an appreciable effect on the internal surface area, it would have to increase it by about 5 m^2 per cm^3 of material. Since the volume of the microcracks does not normally exceed 0.001 (Eq. 38), the width of the microcracks would thus have to be $0.001/50000 = 2\times10^{-8}$ cm and their spacing would have to be at most 2×10^{-8} cm/$0.0006 = 3\times10^{-5}$ cm for the contribution of microcracking to internal surface area to be significant. At such a small spacing we could hardly speak of microcracks but of breakage of the bonds in the microstructure. So, microcracking due to drying cannot appreciably influence the internal surface areas.

Effect of Cracking on Moisture Diffusivity

As one consequence of cracking, we may suspect an increase in the permeability of concrete to water and an increase in the drying rate. To allow estimating this effect, let us assume the cracks to be continuous, planar, parallel, and of constant opening width w, and consider a uniform velocity

field of seepage flow parallel to the cracks. The flow velocity may be assumed to be so low that no turbulence arises (low Reynolds number). Water may be transferred along the cracks as vapor or as liquid (capillary) water or as adsorbed water. However, only the transfer of vapor can be of significance for typical crack widths, as we shall show later.

The mass flux of vapor along one crack is, according to Poiseuille law, $\underset{\sim}{J}_1 = -(\rho_v/12\ \mu_v)w^3\ \text{grad}\ p_v$, where p_v = partial pressure of water vapor in the air within the crack, ρ_v = mass density of water vapor, and μ_v = viscosity of vapor. The flux per unit area of concrete (kg per m^2 per second) then is $\underset{\sim}{J}_v = \underset{\sim}{J}_1/s$, where s = crack spacing. According to the definition of permeability a_v of vapor through concrete, we have further $\underset{\sim}{J}_v = -(a_v/g)\text{grad}\ p_v$, where g = gravity acceleration (9.806 m/s^2). Comparison then yields

$$a_v = \frac{\rho_v g}{12\mu_v}\frac{w^3}{s}\ . \tag{39}$$

From the condition of conservation of mass of water, $\partial W/\partial t = -\text{div}\ \underset{\sim}{J}_v$, where W = water content (m^3 per kg of concrete). Substitution for $\underset{\sim}{J}_v$ then yields the diffusion equation $\partial W/\partial t = (a_v/g)\text{div grad}\ p_v$, which may be also written as $\partial h/\partial t = C_v\ \text{div grad}\ h$, where $h = p_v/p_s$ and C_v = diffusivity = $(a_v/g)\partial p_v/\partial W$. Consequently, the diffusivity of water due to vapor flow in the cracks may be expressed as:

$$C_v = c_v\frac{w^3}{s},\quad \text{with}\ c_v = \frac{\rho_v}{12\mu_v}\frac{p_s}{W_1}\frac{\partial h}{\partial \bar{W}} \tag{40}$$

in which $\bar{W} = W/W_1$ = relative water content, W_1 = water content W at saturation.

To make numerical estimates, the derivative $\partial h/\partial\bar{W}$, which represents the slope of the desorption isotherm of concrete, may be estimated as 1.5. Let us consider h = 0.75 and temperature 20°C (T = 293°K). The mass density of saturated vapor at 20°C is 21.6 g/cm^3, from which we get ρ_v = 13.0 g/m^3 for air-vapor mixture at h = 0.75. Also $\mu_v = 180\times10^{-6}$ g/cm sec, p_s = 2338 N/m^2. Assume that 7% of the weight of concrete is evaporable water, i.e., $W_1 = 0.07\times 2400$ kg/m^3, and that the width of the cracks is w = 0.3 mm and their spacing is s = 30 cm. Eq. (40) then yields

$$C_v \approx 98\quad cm^2/\text{day}. \tag{41}$$

For comparison, the typical diffusivity of intact structural concrete at age 28 days is roughly 0.1 cm^2/day. So, according to Eq. (40), the cracks that we considered increase the drying diffusivity about 1000 times. For shrinkage cracks of width 0.01 mm, the increase of the diffusivity is only about twice and for thinner cracks the effect on drying is negligible.

Since $w \approx s\Delta\varepsilon_{sh}$ (Eq. 29), the diffusivity C_v is approximately proportional to w^2 or to s^2. And because approximately s = 0.5 D, we have

$$C_v \approx \frac{c_v}{4}\Delta\varepsilon_{sh}^3\ D^2 \tag{42}$$

where D = depth of penetration of drying. This shows that at the beginning of drying the effect of cracking on the rate of drying should be negligible. But later, as the cracks get deeper and more widely spaced, the effect may become tremendous.

The foregoing estimates must be understood as upper bounds. Due to crack roughness, thickness variation and tortuosity of flow passages, the increase

of diffusivity will be somewhat less than the foregoing formulas indicate, although of the same order of magnitude. Furthermore, if the cracks are discontinuous, the increase of diffusivity can be offset by several orders of magnitude and can become negligible. From observations we presently know next to nothing about crack continuity. However, it is clear that the thinner the crack the more likely is its discontinuity. Perhaps cracks over 0.3 mm can be safely assumed as continuous and those under 0.01 mm as discontinuous, but further studies are needed.

Cracks in unsaturated concrete can be filled by capillary water only if the diameter $2R_c$ of capillary meniscus is not less than the crack width w. Noting that the capillary meniscus in a planar crack must be cylindrical, and using the Kelvin equation, we have $2\gamma_w \geq -p_c w$, where γ_w = surface tension of water in air (γ_w = 72.8 dyne/cm at 20°C). According to the ideal gas approximation for vapor, the condition for thermodynamic equilibrium is known to yield the pressure of capillary water $p_c = \ell n h \rho_w RT/M$ where R = gas constant, M = molecular weight of water, T = absolute temperature. For 20°C (293°K) $\rho_w RT/M$ = 135 N/mm^2. So, for the crack to be filled by capillary water

$$w \leq \frac{2\gamma_w}{-\ell n\ h} \frac{M}{\rho_w RT} \tag{43}$$

For h = 0.99 we get $w \leq 1.08\times10^{-4}$ mm, and for h = 0.9 we get $w \leq 1.02\times10^{-5}$ mm. The width of continuous cracks always exceeds these values by far. So, the transfer of liquid (capillary) water along the cracks is irrelevant for drying. It is of course relevant for seepage of water through concrete under higher than atmospheric pressure, and in analogy to Eq. (39) the corresponding permeability is

$$a_w = \frac{\rho_w g}{12\mu_w} \frac{w^3}{s} \tag{44}$$

where ρ_w = 1 g/cm^3, μ_w = 0.01002 g/cm sec (at 20°C). This equation indicates that a_w is about 830 times larger than a_v at the same w and s.

Principal Conclusions

1. To be certain that drying of test specimens causes no cracking or microcracking, the differences in pore humidity (relative vapor pressure) within the specimen should not exceed about 2% (Eq. 5).

2. In case of sudden exposure to a drying environment, the wall thickness would have to be unreasonably small (below 0.1 mm) in order to assure that no cracks or microcracks are produced (Eq. 17).

3. Cracking can be avoided if the environmental humidity is decreased gradually and sufficiently slowly. However, the specimens have to be unreasonably thin (about 1 mm) to make this approach possible. Cracking can of course be also eliminated by loading which produces sufficient triaxial compression.

4. Drying normally produces systems of parallel cracks whose spacing and width are approximately proportional to the depth of penetration of drying. In the usual test specimens, the cracks are usually too thin to be visible by unaided eye (Eq. 27).

5. In normal size test specimens, drying is more likely to produce discontinuous microcracking than continuous macrocracks. The microcracking is appropriately modeled as tensile nonlinearity with strain softening (Fig. 7) rather than a sudden drop of stress.

6. Shrinkage cracking can increase the drying diffusivity by several orders of magnitude. During the process of drying, the effect of cracks on the drying rate is at first negligible but can strongly increase as the cracks become deeper. The increase, if any, is roughly proportional to the square of crack spacing or to the square of the depth of penetration of drying.

Acknowledgment

Financial support under U.S. National Science Foundation Grant Number CME8009050 is gratefully acknowledged.

References

1. Z. P. Bažant, S. T. Wu, "Creep and Shrinkage Law for Concrete at Variable Humidity," Journal of the Engineering Mechanics Division, ASCE, 100, 1183-1209 (1974).

2. J. Becker, B. Bresler, "Reinforced Concrete Frames in Fire Environments," Journal of the Structural Division, ASCE, 103, 211-224 (1977).

3. F. Wittmann, P. Roelfstra, "Total Deformation of Loaded Drying Concrete," Cement and Concrete Research, 10, 601-610 (1980).

4. Z. P. Bažant, L. Panula, "Practical Prediction of Time-Dependent Deformations of Concrete," Materials and Structures (RILEM, Paris), Parts I & II 11, 307-328 (1978); Parts III and IV, 11, 415-434 (1978); Parts V and VI, 12, 169-183 (1979).

5. Z. P. Bažant, L. Najjar, "Nonlinear Water Diffusion in Nonsaturated Concrete," Materials and Structures (RILEM, Paris), 5, 3-20 (1972).

6. H. S. Carslaw, J. C. Jaeger, Conduction of Heat in Solids, Clarendon Press, 2nd ed., 102-105, 198-201 (1959).

7. S. V. Aleksandrovskii, Analysis of Concrete Structures at Variable Temperature and Humidity with Account of Creep (in Russian), Stroyizdat, Moscow (1973).

8. P. Klug, "Kriechen, Relaxation und Schwinden von Zementstein," Dissertation, Technische Universität, München (1973).

9. Z. P. Bažant, A. Asghari, J. Schmidt, "Experimental Study of Creep of Hardened Portland Cement Paste at Variable Water Content," Materials and Structures (RILEM, Paris), 9, 279-290 (1976).

10. S. Chatterji, N. Thaulow, P. Christensen, "Formation of Shrinkage Cracks in Thin Specimens of Cement Paste," Cement and Concrete Research, 11, 155-158 (1981).

11. Z. P. Bažant, H. Ohtsubo, "Stability and Post-critical Growth of a System of Cooling or Shrinkage Cracks," Intern. J. of Fracture, 15, 443-456 (1979).

12. Z. P. Bažant, A. B. Wahab, "Instability and Spacing of Cooling or Shrinkage Cracks," Proc. ASCE, 105, 873-889 (1979).

13. Z. P. Bažant, H. Ohtsubo, 'Stability Conditions for Propagation of a System of Cracks in a Brittle Solid," Mechanics Research Communications, 4, 353-366 (1977).

14. Z. P. Bažant, A. B. Wahab, "Stability of Parallel Cracks in Solids Reinforced by Bars," Intern. J. of Solids and Structures, 16, 97-105 (1980).

15. M. Wecheratana and S. P. Shah, "Resistance to Crack Growth in Portland Cement Composites," Report, Dept. of Material Engineering, Univ. of Illinois at Chicago Circle (1980).

16. S. Mindess, F. Lawrence, C. Kesler, "The J-Integral as a Fracture Criterion for Fiber Reinforced Concrete," Cement and Concrete Research, 7, 731-742 (1977).

17. P. E. Petersson, "Fracture Energy of Concrete: Method of Determination," Cement and Concrete Research, 10, 78-89 (1980), and "Fracture Energy of Concrete: Practical Performance and Experimental Results," Cement and Concrete Research, 10, 91-101 (1980).

18. M. F. Kaplan, "Crack Propagation and the Fracture of Concrete," ACI Journal, 58, 591-609 (1961).

19. Z. P. Bažant, J. H. Heman, H. Koller, L. J. Najjar, "A Thin-Wall Cement Paste Cylinder for Creep Tests at Variable Humidity and Temperature," Materials and Structures (RILEM, Paris), 6, 277-280 (1973).

20. S. Mindess, S. Diamond, "A Preliminary SEM Study of Crack Propagation in Mortar," Cement and Concrete Research, 10, 509-519 (1980).

APPENDIX

Series solution for one-dimensional linear diffusion through a wall (solid bounded by parallel planes) for domain $-a/2 < x < a/2$ (wall), $t_0 = 0$ (drying starts at $t = 0$), h_0 = initial pore humidity, surface humidity $h = h_0 + kt$:

$$h(x,t) = h_0 + kt + \frac{k}{2C}\left(x^2 - \frac{a^2}{4}\right) + \frac{4ka^2}{\pi^3 C}\sum_{n=0}^{n=\infty}\frac{(-1)^n}{(2n+1)^3}\exp\left[\frac{-C(2n+1)^2\pi^2 t}{a^2}\right]\cos\left[\frac{(2n+1)\pi x}{a}\right]. \qquad (45)$$

If drying stops at $t = t_1$, i.e., the surface humidity is constant for $t \geq t_1$, then, by superposition,

$$h(x,t) = h_0 + kt_1 + \frac{4ka^2}{\pi^3 C}\sum_{n=0}^{n=\infty}\frac{(-1)^n}{(2n+1)^3}\cos\left[\frac{(2n+1)\pi x}{a}\right]\left(\exp(\alpha_n t) - \exp[\alpha_n (t - t_1)]\right) \qquad (46)$$

$$\alpha_n = \frac{-C(2n+1)^2\pi^2}{a^2}.$$

Series solution for linear diffusion (axisymmetric) in a solid cylinder, $0 < r < a$; $h(r,0) = h_0$, $h(a,t) = h_0 + kt$:

$$h(r,t) = h_0 + k\left(t - \frac{a^2 - r^2}{4C}\right) + \frac{2k}{aC}\sum_{n=1}^{\infty} \exp(-C\beta_n^2 t)\,\frac{J_0(r\beta_n)}{\beta_n^3 J_1(a\beta_n)} \,. \tag{47}$$

If drying stops at $t = t_1$, then, by superposition:

$$h(r,t) = h_0 + kt_1 + \frac{2k}{aC}\sum_{n=1}^{\infty} \frac{J_0(r\beta_n)}{\beta_n^3 J_1(a\beta_n)}\left[\exp(-C\beta_n^2 t) - \exp(-C\beta_n^2 (t - t_1))\right] \tag{48}$$

where J_0 = Bessel function of the first kind, order 0;
J_1 = Bessel function of the first kind, order 1;
$a\beta_n$ = roots of J_0.

Implicit finite difference equation for linear diffusion in a cylinder, Crank-Nicolson Method, Δr = nodal spacing, i = 1,2,3,...=node numbers:

$$\left(\frac{r}{\Delta r^2} - \frac{1}{2\Delta r}\right)h_{i-1}^{+} + \left(\frac{-2r}{\Delta r^2} - \frac{2r}{C\Delta t}\right)h_i^{+} + \left(\frac{r}{\Delta r^2} + \frac{1}{2\Delta r}\right)h_{i+1}^{+}$$

$$= -\left\{\left(\frac{r}{\Delta r^2} - \frac{1}{2\Delta r}\right)h_{i-1} + \left(\frac{-2r}{\Delta r^2} + \frac{2r}{C\Delta t}\right)h_i + \left(\frac{r}{\Delta r^2} + \frac{1}{2\Delta r}\right)h_{i+1}\right\} \tag{49}$$

but the finite difference equation for the node at the center of cylinder (r = 0) must be based on rectangular coordinates:

$$-2\left(1 + \frac{\Delta r^2}{C\Delta t}\right)h_0^{+} + 2h_1^{+} = -\left\{-2\left(1 - \frac{\Delta r^2}{C\Delta t}\right)h_0 + 2h_1\right\}. \tag{50}$$

h_i^{+} are the nodal unknowns to be solved; h_i are known values from previous time step.

Finite difference equation for nonlinear diffusion using Lees' Method (3 time levels):

$$r\,\frac{h_i^{+} - h_i^{-}}{2\Delta t} = \left[\frac{C_{i+1} - C_{i-1}}{4\Delta r^2/r} + C_i\left(\frac{1}{2\Delta r} + \frac{r}{\Delta r^2}\right)\right]h_{i+1} - \frac{2C_i r}{\Delta r^2}\,h_i$$

$$+ \left[C_i\left(\frac{1}{2\Delta r} + \frac{r}{\Delta r^2}\right) - \frac{(C_{i+1} - C_{i-1})r}{4\Delta r^2}\right]h_{i-1} \tag{51}$$

$$\text{Replace} \begin{cases} h_{i+1} & \frac{1}{3}(h_{i+1}^{+} + h_{i+1} + h_{i+1}^{-}) \\ h_i \quad \text{with} & \frac{1}{3}(h_i^{+} + h_i + h_i^{-}) \\ h_{i-1} & \frac{1}{3}(h_{i-1}^{+} + h_{i-1} + h_{i-1}^{-}) \end{cases}; \tag{52}$$

group terms so as to obtain $[A]\{h^{+}\} = \{b\}$ with $\{b\}$ vector consisting of known h and h^{-} terms as well as boundary h^{+} terms. A modification similar to Eq. (50) is required at the center for solid cylinders.